



Power Biomass to Liquid — an option for Europe's sustainable and independent aviation fuel production

Felix Habermeyer¹ · Julia Weyand¹ · Simon Maier¹ · Esa Kurkela² · Ralph-Uwe Dietrich¹

Received: 12 October 2022 / Revised: 11 December 2022 / Accepted: 13 December 2022
© The Author(s) 2023

Abstract

The European Union guides its member states to a gradual uptake of sustainable aviation fuel (SAF) from 2% vol. in 2025 to 63% vol. by 2050 with the ReFuelEU proposal as part of the Fit-for-55 package. A promising production pathway for SAF presents itself in the Power Biomass to Liquid (PBtL) process, which converts non-crop-based biomass residue and renewable power via the Fischer–Tropsch route. In this study, a techno-economic and greenhouse gas (GHG) emission analysis of a small-scale (50 MW_{th}) PBtL process concept, developed in the EU project FLEXCHX, is presented. The analysis is conducted with a thermodynamic process model implemented in Aspen Plus[®], which relies on experimental project data. For the PBtL base case production costs of 1.09 €₂₀₂₀/l are estimated, whereby electricity and investment into the alkaline electrolyzer constitute the largest cost drivers. At low electricity prices (< 39.2 €/MWh), the PBtL process is more cost effective than the reference process Biomass to Liquid (BtL). To identify improvements to the base case design, different design options are considered under varying economic boundary conditions: Solid oxide electrolysis is more economic than alkaline electrolysis at higher electricity prices due to its higher system efficiency. Maximizing the product yield by increased CO₂ recycling is only economically reasonable below an electricity price threshold, which is found at 20 €/MWh for the base case. Further, PBtL is heavily dependent upon the availability of low GHG electricity in order to produce SAF with a low carbon footprint. Assuming full utilization of the EU's non-crop-based biomass residues, the EU jet fuel demand for 2030 could be met with the PBtL process.

Keywords Power and Biomass to Liquid · Biomass to Liquid · Fischer–Tropsch · Techno-economic analysis · Alkaline electrolysis

Abbreviations

ACC	Annual capital cost	HEFA	Hydrotreated ester and fatty acids
AEL	Alkaline electrolysis	HPS	High pressure steam
AR	Agricultural residue	HRSG	Heat recovery steam generation
ASU	Air separation unit	IR	Interest rate
BtL	Biomass to Liquid	LCA	Life-cycle assessment
CAPEX	Capital expenditures	LPS	Low pressure steam
CW	Cooling water	LR	Long recycle
DME	Dimethyl ether	MPS	Medium pressure steam
FCI	Fixed capital investment	NPC	Net production cost
FR	Forrest residue	OPEX	Operational expenditures
FT	Fischer-Tropsch	PBtL	Power Biomass to Liquid
		PEM	Proton exchange membrane
		PL	Plant lifetime
		PV	Photovoltaic
		RF	Refrigeration
		RWGS	Reverse water gas shift
		SAF	Sustainable aviation fuel
		SBCR	Slurry bubble column reactor
		SNG	Synthetic natural gas
		SOEC	Solid oxide electrolysis cell

✉ Felix Habermeyer
felix.habermeyer@dlr.de

¹ DLR e.V., Deutsches Zentrum für Luft- und Raumfahrt, Stuttgart, Germany

² VTT Technical Research Centre of Finland Ltd., Teknologian Tutkimuskeskus VTT Oy, Espoo, Finland

SR	Short recycle
SRR	Short recycle with reformer
SXB	Staged fixed bed
WHSV	Weight hourly space velocity

Symbols

R	Reaction rate
k	Kinetic constant
K	Equilibrium constant
α	Chain growth probability
DENOM	Denominator
LHV	Lower heating value
HHV	Higher heating value
P	Price
AC	GHG abatement cost

1 Introduction

Towards its goal of reaching 55% GHG-emission reduction by 2030, the EU has passed the legislative package Fit-for-55 [1]. The package contains the ReFuelEU proposal introducing measures for GHG reduction in the aviation industry [2]. Along with other measures, ReFuelEU mandates a gradual ramp-up of sustainable aviation fuel (SAF) blending from 2% vol. in 2025 to 63% vol. by 2050. Similarly, the US government targets a SAF production increase to 3 billion gallons per year until 2030 [3]. SAF is currently the most promising option for replacing fossil jet fuel due to its high energy density compared to other forms of energy provision such as battery or hydrogen storage. Yet, an optimal SAF production route remains a topic of discussion as many aspects, including production cost, GHG-footprint or the possible production volume in the EU, have to be considered.

A variety of feedstock and process types have been proposed for the production of SAF. E-fuel routes convert CO₂ from industrial point sources or direct air capture to SAF. The advantage of biomass-based routes over e-fuels is the lower energy demand for the feedstock reduction. Besides biomass routes that rely on oils (HEFA), sugar or algae, lignocellulose biomass offers a comparatively large feedstock base, for which a number of conversion routes have been established [4]. The Fischer–Tropsch (FT) route is a mature process with many commercial plants running on coal today and several biomass based project plants [5]. In addition, the FT route is estimated to have lower production cost for large-scale plants than alternative lignocellulose biomass routes, such as alcohol to jet (AtJ) or the synthesized iso-paraffine (SiP) route [4]. Yet, the FT route, also referred to as Biomass to Liquid (BtL), is limited in its carbon conversion [6]. Accordingly, it has been argued that BtL can only contribute a fraction of the EU's SAF demand [7]. Here, relying on the conversion of renewable electricity and non-crop-based

biomass, the Power Biomass to Liquid (PBtL) process offers a promising solution for the large scale low-emission production of SAF. The addition of electrolytic hydrogen while recycling CO₂ generated in the process enables a nearly full conversion of the limited biogenic carbon to hydrocarbon chains [6].

Several techno-economic studies on the PBtL process have been published: Hillestad et al. [8] find production cost of 1.7 \$/l for a PBtL process with 435 MW_{th} biomass input assuming an electricity price of 50 \$/MWh. Thereby, a carbon efficiency of 91% is reached by nearly full carbon recycling. Albrecht et al. estimate production costs of 2.15 €/l_{GasolineEquivalent} at an electricity price of 105 €/MWh [6]. Here, the PBtL plant with an output of 240 kt/year has a carbon efficiency of 97.7%. Isaacs et al. assess local PBtL production costs for the eastern part of the USA based on local biomass prices and PV and wind availability [9]. For every location, an off-grid electrolysis and energy storage system is optimized to produce a constant hydrogen stream at minimal cost. For the year 2030, the most economic product quartile is estimated to have a minimum selling price of 2.40 \$₂₀₃₀/l for systems operated with PV and wind as their power sources.

Other PBtL studies aim to find process designs for optimal technical efficiency. Nielsen et al. simulate a novel PBtL process concept in which an SOEC is partially fed by FT off-gas [10]. Based on their detailed simulation of the SOEC unit, the PBtL process' energy efficiency is hypothesized to reach 90% at a carbon efficiency of 91%. Dossow et al. discuss different process designs for a PBtL concept operated with a PEM electrolyzer [11]. With a hydrogen addition of 0.24 t_{H₂}/t_{fuel}, the process is estimated to reach a carbon efficiency of 97%.

The principle of adding electrolytic hydrogen to biomass derived syngas can also be used for other products than Fischer–Tropsch fuel. Here, products like SNG [12, 13], methanol [14, 15] or methanol to gasoline [13], ethanol [14], and DME [16] can be found in literature.

A number of studies include an LCA in their discussion of the PBtL process. Bernical et al. perform a comparative study on PBtL and BtL considering GHG impact and production costs of both processes [17]. The PBtL concept producing hydrogen with a SOEC system is found to be the more efficient concept, with higher fuel yield and similar economics and emissions, when electricity with a GHG footprint lower than 150 g_{CO₂,eq}/kWh is available. Koponen and Hannula [18] conduct a comparative LCA study for the processes presented in Hannula [13]. Here, the outsized role of green electricity for the production of low GHG fuels is emphasized as well.

In the EU project FLEXCHX, a small-scale hybrid BtL-PBtL plant (50 MW_{th}) has been investigated [19]. The project concept relies on the idea of the plant switching

operation mode between BtL and PBtL depending on the situation on the energy market. When inexpensive and low GHG electricity is available, an electrolysis unit is switched on to boost the fuel output of the system. Otherwise, the plant can be run in BtL mode, where the electrolyzer is turned off, and the oxygen for gasification is provided by an ASU. To facilitate the small-scale and hybrid operation, a staged fixed bed (SXB) gasifier [20] in combination with a novel syngas cleaning system [21] have been developed and experimentally analyzed in a 1 MW pilot plant throughout the project. Similarly, the Winddiesel project successfully showcased the operation of an 8 MW_{th} PBtL plant with a dynamic H₂ hydrogen input [22]. Further, Shell has presented plans to build a PBtL plant at the Rhineland refinery. An already installed 10 MW_{el} PEM electrolyzer will be scaled up to 100 MW_{el} to provide the necessary hydrogen for this plant [23].

The aim of this study is to evaluate the possible role of PBtL for the EU aviation sector. To that end, production cost, GHG emissions and production capacity in the EU are estimated. The same analysis is conducted for the BtL process, which serves as a reference case. Both process models are derived from the 50 MW_{th} steady-state FLEXCHX process concept. The unit models are based on experimental project data. In order to avoid an overestimation of the production cost, different PBtL process designs are discussed under varying economic boundary conditions. A similar comprehensive techno-economic and ecologic approach to this novel process scheme and the discussion of its process design options has not been published yet. With that, it can be shown how the key advantage of the PBtL process, its higher product yield, can be utilized for SAF provision in the EU depending on national economic boundary conditions.

2 Methodology

2.1 Power Biomass to Liquid

The super-structure flowsheet, as depicted in Fig. 1, includes all process units needed for the conversion of biomass to FT product. Additionally, the flowsheet contains all process

design options, which will be discussed in the following sections.

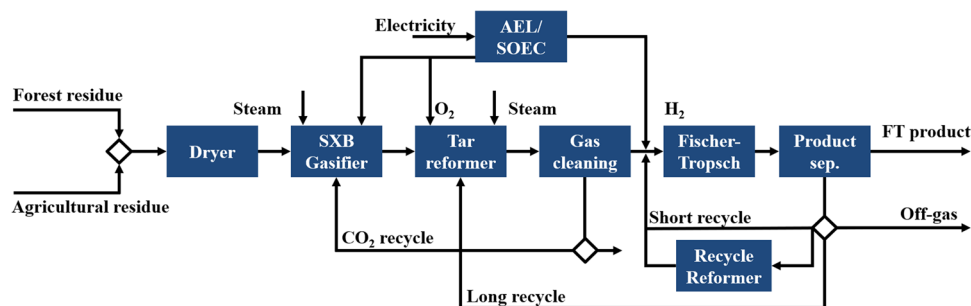
This flowsheet is conceptualized for a small-scale application with 50 MW_{th} biomass input. Compared to larger plants that rely on the economy-of-scale effect for low production costs, this concept has mainly two advantages: small-scale biofuel production only requires a limited biomass transport radius. This leads to lower greenhouse gas emissions and lower cost for the biomass transport. Secondly, second generation biofuel plants are not in industrial use to date. This can be attributed to the high investment cost for a first-of-a-kind plant. To that end, small-scale plants can lower the financial risk for the initial investment [20]. However, lower total investment costs, lower material use for the plant construction, and a more seamless integration into the refinery infrastructure might persuade investors to switch to larger plant sizes later.

The initial wet biomass is introduced into an air dryer. Only low-grade heat is needed for air drying [24], which is readily available from the exothermal PBtL process. Therefore, air drying is preferred over steam drying in this study. Additional pre-treatment steps, such as torrefaction or pelleting [25], are not considered in this study, as they are not necessarily required for an SXB gasifier. These steps increase the biomass LHV and subsequently the process yield. This delta in yield would have to be weight against additional investment and operation costs for these pre-treatment steps.



The dried biomass is converted to syngas in a staged fixed bed gasifier (SXB). With the addition of steam, recycled CO₂ and oxygen, the complex biomass molecules can be cracked into a product gas phase containing mainly CO, H₂, CO₂, and steam as well as contaminant components such as tars, CH₄, H₂S, and NH₃. For gasifier and reformer, all syngas components can be assumed to be in chemical equilibrium according to the water gas shift reaction in Eq. (1) [26]. The SXB gasifier technology is applied in this concept due to its lower capacity range compared to entrained flow and fluidized bed gasification, which are typically used for plants with > 100 MW_{th} biomass input [20].

Fig. 1 PBtL super-structure process flowsheet. Design options are signified by diamond shapes (◇)



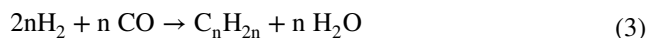
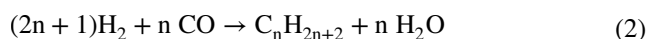
Tars formed in the gasifier have to be removed due to their detrimental effect to the subsequent process steps, especially the FT catalyst. Here, catalytic tar reforming is chosen for its higher H_2 and CO yield compared to thermal tar cracking. Thermal cracking requires higher temperatures (1100–1300 °C) than catalytic reforming (700–900 °C) [27]. For autothermal operation, higher temperatures can only be attained by oxidizing a larger part of the syngas and thereby losing fuel efficiency.

Not all contaminants that would act as catalyst poison in the FT reactor can be removed in the tar reformer. Therefore, additional gas cleaning steps are comprised in the gas cleaning section in Fig. 1. A novel adsorption-based gas cleaning system is studied here. This system is experimentally proven in conjunction with an SXB gasifier and an FT reactor [21]. Additionally, this technology is advantageous for small scale plants compared to conventional wet scrubbing technologies, such as Selexol or Rectisol, due to its simpler operation and reduced need for adsorbent replacement [21].

CO_2 removed from the syngas stream by a water scrubber is partly recycled to the SXB gasifier. This will improve the overall carbon conversion. Alternative measures to increase the process carbon conversion, e.g., the addition of hydrogen to gasifier or reformer stage [6, 8], are not studied here. The CO_2 recycling option appears to be most suitable for this concept because CO_2 can substitute steam as gasification medium [20].

Syngas from the gas cleaning section has a H_2/CO ratio below the stoichiometric ratio of 2.1, especially when CO_2 is recycled. Hydrogen from the electrolyzer unit is added to the syngas prior to the FT reactor to attain the stoichiometric reactant ratio. Additionally, the electrolytically produced oxygen can be used in gasifier and reformer.

In the FT reaction, hydrogen and carbon monoxide are converted to long-chained hydrocarbons. The main reactions are the conversion to paraffine (Eq. 2) and olefin (Eq. 3) [28].



For this concept, a low temperature Fischer–Tropsch reaction over a cobalt catalyst is applied. Its high selectivity for the product fraction C_{5+} sets it apart from the high temperature FT reaction [28]. The slurry bubble column reactor is selected as the reactor type rather than fixed bed or microreactor [5]. Advantages of the slurry bubble column are its high thermal stability and low investment cost [29].

The FT product is separated from short hydrocarbon molecules C_{1-4} , unconverted reactants and the produced water. The hydrocarbon byproducts C_{1-4} together with the unconverted reactants are recycled to the process in order to increase the product yield. In order to avoid inert gas

accumulation in the process, a fraction of the gas stream has to leave the process as off-gas. The off-gas is subsequently burned and considered in the heat integration.

2.2 Design options

2.2.1 Biomass feedstock

Biomass feedstock for the PBtL process can be broadly categorized into forestry and agricultural residue. First generation biofuels produced from food or animal feed crops are not included in this study. The advantage of focusing only on second generation biofuels is that their production is not in competition with food production [30].

The high availability of agricultural residue is a strong argument for its utilization for fuel production. In the EU, an annual availability of 139 Mt_{dry} is estimated [31]. Whereas, forest residue has an annual potential of 40 Mt_{dry} [31]. Yet, forest residue can be converted to fuel with less technical effort in the syngas cleaning section. The on average higher level of contaminants in agricultural biomass can only be reduced with a more energy-intense syngas cleaning in this process concept [20]. For both biomass types, continuous supply throughout the year is assumed.

The availability values used here can be seen as a rough benchmark. Studies on the biomass availability diverge in their estimated ranges. Searle and Marlins state a forest residue potential of 67 Mt_{dry}/a . When considering biomass retention for soil quality, only 21.53 Mt_{dry}/a remain [32]. Of the total agricultural residue of 315.9 Mt_{dry}/a remain 119.8 Mt_{dry}/a after subtracting the retention value [32]. Panoutsou and Maniatis find a forest residue availability of 41–68 Mt_{dry}/a in 2030 [33].

2.2.2 Fischer–Tropsch off-gas recycle

An FT off-gas recycle is employed to increase the process product yield. Only a limited fraction of the hydrogen and carbon monoxide in the FT input stream can be converted to liquid product in a once-through operation [34]. A higher carbon conversion for the process can be attained by recycling the unconverted syngas. Here, different recycling options can be employed. In this work, three recycling options, as depicted in Fig. 1, are discussed.

The long recycle (LR) reintroduces the FT off-gas into the reformer. This allows the reforming of the short-chained hydrocarbon gas fraction C_{1-4} . However, the long recycle needs to be heated up to the reformer temperature, typically 700–900 °C [27]. As an autothermal reformer is considered in this concept, energy for the temperature increase can only be provided by oxidizing part of the syngas stream. This, in turn, shifts the overall process yield from the product

towards CO₂ and steam. This option has been discussed in literature by several sources [35, 36].

The short recycle (SR) leads the off-gas stream to the FT inlet. Here, the recycle stream only needs to be heated up to the FT temperature, which in this concept is distinctly lower than the reformer temperature. In addition, the already clean FT off-gas stream does not have to be led through the syngas cleaning section. The short recycle has been studied in combination with a long recycle by Hillestad et al. [8].

For the short recycle reformer (SRR) option, an additional reforming stage is added in the short recycle loop. Thereby, the short-chained hydrocarbon gas fraction C₁₋₄ can be reformed while an unnecessary pass through the syngas cleaning section can be avoided. This saves capital and operational expenses in the gas cleaning section. Yet, these savings have to be weighed against the cost for the additional reformer.

2.2.3 Electrolysis technology

The electrolytic splitting of water into hydrogen and oxygen can be accomplished via different technology options. Here, the alkaline electrolysis (AEL) is compared with the solid oxide electrolysis cell (SOEC) technology.

The alkaline electrolysis has the highest technology readiness level of all currently available electrolysis technologies [37]. The largest AEL system currently installed has a reported capacity of 10 MW_{el} [38]. Accordingly, investment costs for this technology are low compared to other electrolysis technology options [37, 39].

Although SOEC technology has the lowest technological development level, its high electric efficiency promises low operation costs. SOEC systems are commonly operated at a high temperature range of 700–900 °C, opposed to 60–90 °C for AEL. At this temperature range, a large part of the reaction enthalpy can be covered by thermal instead of electrical energy [37].

Both technologies have drawbacks in the context of high-pressure and highly dynamic applications. A proton exchange membrane (PEM) electrolyzer is more suitable for these operation conditions. Pressures up to 50 bar can be handled by a PEM electrolyzer, while the typical pressure range for AEL systems only operate up to 30 bar [37].

Similarly, its low start-up time and high load flexibility makes PEM the preferred technology over AEL and SOEC when operating the electrolyzer under flexible load [37].

2.2.4 CO₂ recycle rate

CO₂ is removed from the syngas stream in the gas cleaning section via a pressurized water scrubber [21]. The removed CO₂ can be reintroduced into the SXB gasifier. Here, CO₂ can replace steam as a dilution medium for oxygen [40]. A higher CO₂ recycle rate leads to a higher carbon conversion and, consequently, a higher total product yield. However, it also prompts a higher hydrogen demand to fix the H₂/CO ratio to the stoichiometric value of 2.1. As a consequence, the higher product yield has to be weighed against the additional electricity demand for the electrolyzer.

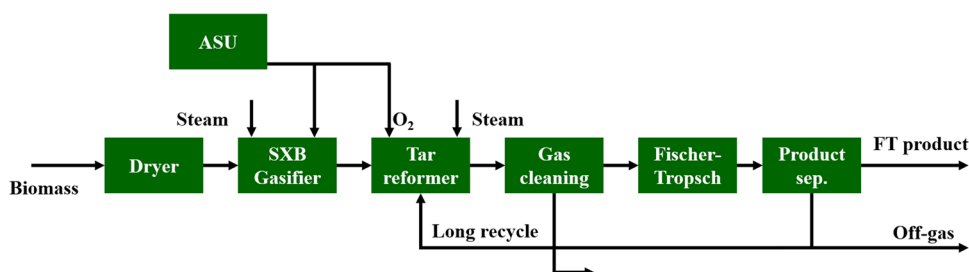
2.3 Biomass to Liquid

To have a reference case, the PBtL process is simulated alongside the BtL process [6]. In contrast to the PBtL process, no electrolyzer is utilized for the conversion of biomass to FT fuel in the BtL process. This lowers the product yield. Yet, investment for the electrolyzer and the connected electricity cost can be omitted.

The BtL process flowsheet can be taken from Fig. 2. The unit sequence from dryer to product separation relies on the same technology as the PBtL process, with two notable exceptions: Firstly, the BtL process has no CO₂ recycle. The stoichiometric H₂/CO ratio for the FT reaction is adjusted by steam addition in the gasifier and reformer. Steam addition shifts the chemical equilibrium in the water gas shift reaction towards H₂ while depleting CO (cf. Equation 1). Secondly, the oxygen for reformer and gasifier has to be produced in an air separation unit (ASU) since no electrolyzer is used in the BtL process.

An ASU was chosen here, as it is the most mature technology for the separation of oxygen. Adsorption and chemisorption based solutions should be monitored as alternative solutions as their technical maturity increases [41]. Especially for applications with a low oxygen demand, these solutions can be favorable. Air separation units have an economic application range higher than 20 sTPD (short

Fig. 2 BtL flowsheet



tons per day sTPD) [41]. Yet, for this BtL process concept an oxygen production of 155 TPD (171 short tons per day sTPD) is required.

2.4 Process model

The process analysis is based on a flowsheet simulation implemented in Aspen Plus® (V10). A super-structure model containing the two paths, PBtL and BtL, along with the described process design options is modeled. DLR's software tool TEPET enables the selection of path and process design with a subsequent automated techno-economic-ecological process analysis [42]. More specifically, a set of simulation parameters are specified in TEPET. The program then runs simulations with the specified parameters and automatically retrieves the simulation results from Aspen Plus®. With the results, an automated utility integration is conducted before the techno-economic and GHG emission analysis can be performed. This allows for the rapid analysis of various process designs.

For the Aspen Plus flowsheet, the Soave–Redlich–Kwong equation of state is used [13], which is the recommended property method for hydrocarbon processes [43]. In the following sections, crucial modeling parameters are discussed in detail. Further assumptions can be found in the Supplementary Material.

All technical and economic modeling assumptions underlie different levels of uncertainty. Economic assumptions are almost all subject to price fluctuations, whereas technical parameters, such as the availability of biomass residues or the electrolyzer efficiency, are affected by macro-economic or technical developments. To ensure the validity of the statements derived from the simulation results, a sensitivity study is conducted for the most important parameters. To assess the uncertainty regarding the results further, methods such as the global sensitivity and uncertainty analysis could be applied in future work [44].

2.4.1 Feedstock model

To make a broader statement about the entire forest and agricultural residue, two representative feedstocks are chosen. Their respective properties can be found in Table 1. The total set of forest residue is represented by wood pellets as analyzed by Kurkela et al. [20]. Agricultural residues are simulated with the composition of sunflower husk [20].

2.4.2 Gasification and reforming section

The gasifier is operated at 5 bar and 850 °C. Steam and CO₂ function as the dilution medium for the gasifier's oxygen input. The mass flow of dilution medium is fixed to 1.3

Table 1 Biomass feedstock compositions and thermodynamic properties as modeled in Aspen Plus [20]

Feedstock	Forest residue	Agricultural residue
Proximate analysis, wt. % dry basis		
Fixed carbon	17.1	22.2
Volatile matter	82.5	75
Ash	0.4	2.8
Ultimate analysis, wt. % dry basis		
Ash	0.4	2.8
C	49.8	52.1
H	6.3	5.8
N	0.13	0.7
S	0.01	0.14
O (difference)	43.36	38.46
Other properties		
HHV, MJ/kg _{db} , ^a	19.77	19.67
Initial moisture content, wt. %	50	50

^aHHV calculation according to $\text{HHV} = \text{LHV}_{\text{dry}} + 0.02441 \cdot w_{\text{H}_2\text{O}} \cdot (18.015/2.016)$

times the mass of oxygen input. These operation conditions represent set point 20/11B in the SXB test campaign [20].

The CO₂ and steam ratio in the dilution medium is variable in the simulation. The more CO₂ is recycled to the gasifier, the more steam can be replaced by CO₂ as dilution medium. For the base case, as defined in Sect. 2.5, CO₂ makes up 65% of the total dilution stream in accordance with set point 20/11B [20].

The SXB gasifier's hydrocarbon and tar formation, modeled as naphthalene and benzene, are fitted to the experimental results of operation point 20/11B [20]. In Aspen Plus, this is modeled with an RYield reactor. The molecule specific yield can be found in the Supplementary Material.

Syngas components H₂, CO₂, H₂O, and CO react according to the water gas shift equilibrium (Eq. 1). Here, the reaction's equilibrium coefficient describes the ratio of H₂ and CO₂ to H₂O and CO. A higher gasification temperature leads to a lower equilibrium coefficient. During the gasification experiments in the FLEXCHX project, the measured equilibrium coefficients were found to be lower than the theoretical values at the respective gasification temperature. To account for this effect in Aspen Plus, a second reactor stage is modeled using an RGibbs equilibrium reactor. The reactor temperature is set to 950 °C and subsequently cooled down to the actual gasification temperature of 850 °C.

Fly ash, formed in the gasification, is removed by a filter unit following the gasifier. At high temperatures, tar components form soot, which can lead to filter blinding [13, 20]. This is prevented by cooling the gasification syngas prior to the filter unit to 550 °C when agricultural residue serves

as feedstock. Forest residue, with its lower tar formation rate, can enter the filter with the unchanged temperature of 850 °C. Only for cases with a long FT off-gas recycle, a filter temperature of 700 °C is assumed, which accounts for the cooling effect of the recycle.

The autothermal reformer is operated at 750 °C for forest residues and 850 °C for agricultural residues. The higher temperature for agricultural residues is needed for a full conversion of the higher tar content in the syngas. At this temperature a conversion of 80% for CH₄, NH₃, and HCN is assumed [45]. The main components H₂, CO₂, H₂O, and CO are brought into chemical equilibrium with an RGibbs reactor in Aspen Plus. The temperature is adjusted by iterating the oxygen input to the reformer. The oxygen has to be mixed with an equal mass flow of steam to provide the necessary oxygen dilution. For the BtL simulation, the steam addition is iterated to adjust the molar H₂/CO ratio in the reformer product to 2.1. By adding steam to the water gas shift equilibrium (Eq. 1), CO is converted to CO₂ while the H₂ content is increased.

2.4.3 Fischer–Tropsch slurry bubble column reactor

The reaction kinetic by Todici et al. from 2017 is used to describe a continuous stirred tank reactor (CSTR) with Co/Re/γ-Al₂O₃ catalyst loading [46]. The model is based on the carbide mechanism and fitted to experimental data for a temperature range of 478–503 K, a pressure range of 15–25 bar, an H₂/CO ratio in the range of 1.4–2.1 and a weight hourly space velocity (WHSV) in the range of 1–22.5 l_N/(g_{cat} h). N-alkanes and primary alkenes with a carbon chain length up to 30 are considered as product. Equations 4 to 9 give the reaction rate expressions for the kinetic model [46]. Contrary to earlier work by the research group [47, 48], Todici et al. include Eqs. 8 and 9 to account for the secondary 1-olefin hydrogenation kinetic and the secondary pathway for methane formation [46]. Especially for a short recycle process design, the secondary 1-olefin hydrogenation is an important aspect to consider. Unreformed olefins can be re-adsorbed at the FT catalyst and their chain growth may continue. This effect leads to a higher product yield.

$$R_{C_nH_{2n+2}}^{prim} = \frac{k_7 K_2^{0.5} p_{H_2}^{0.5} \alpha_1 \prod_{i=3}^n \alpha_i}{DENOM^2} \quad n \geq 2 \quad (4)$$

$$R_{C_nH_{2n}}^{prim} = \frac{k_{8,0} e^{cn} \alpha_1 \prod_{i=3}^n \alpha_i}{DENOM} \quad n \geq 3 \quad (5)$$

$$R_{C_2H_4}^{prim} = \frac{k_{8E,0} e^{c^2} \alpha_1 \alpha_1}{DENOM} \quad (6)$$

$$R_{CH_4}^{prim} = \frac{k_7 K_2^{0.5} p_{H_2}^{0.5} \alpha_1}{DENOM^2} \quad (7)$$

$$R_{CH_4}^{sec} = \frac{k_M^* P_{CO} P_{H_2}}{DENOM^{*2}} \quad (8)$$

$$R_{C_nH_{2n}}^{*,hyd} = \frac{k_{OHP} C_n H_{2n} K_2^* p_{H_2}}{DENOM^{*2}} \quad n \geq 2 \quad (9)$$

The differential system of equations contains partial pressure expressions of H₂, CO, H₂O (in the denominator terms), and of all 1-olefins in the secondary hydrogenation term (Eq. 9). Therefore, an iterative solution is needed. Since no predefined reaction kinetic model in Aspen Plus fits this problem, a FORTRAN kinetic subroutine is used. The corresponding FORTRAN code can be found in the Supplementary Material. Additionally, a validation of the Aspen model with experimental results from [46] can be found in the Supplementary Material.

In Aspen Plus, the FT reactor is represented by an RCSTR block and operated at 230 °C and 25 bar. High pressure increases selectivity and reaction rate for the FT Co catalyst [28, 46]. Similarly, the highest catalyst activity can be found at high temperatures. Therefore, the highest temperature and pressure are chosen for which the model is still valid. At this operation point, the reactor is assumed to have a CO conversion of 55% [8]. The catalyst mass is iterated to find the defined CO conversion.

2.4.4 Electrolyzer

The two electrolyzer technologies, AEL and SOEC, are modeled with a splitter block operated at 25 bar. The AEL is operated at 60 °C with a system efficiency of 70.8%_{HHV} [37]. For the SOEC technology, a system efficiency of 95%_{HHV} is assumed in thermo-neutral operation [37]. The H₂ and O₂ product streams leave the electrolyzer at 230 °C after recuperation. Pressurized operation of an SOEC system is not technically feasible at the current state due to material restriction. However, it can be assumed that future technological development could make an operation at 25 bar possible [8]. As pressure level and system efficiency are optimistic assumptions, the result should be viewed as a best-case analysis for the SOEC technology.

2.5 Simulation case definition

Table 2 shows the process design configurations for the analyzed cases. A PBtL plant with an AEL, long recycle, and forest residue feedstock is chosen as the base case. This configuration is the most likely design for a first-of-a-kind PBtL plant: The long recycle (LR) is commonly

Table 2 Case definition for the modeled process design options

Case	PBtL (base case)	PBtL-SR	PBtL-SRR	PBtL-SOEC	PBtL _{AR}	BtL
Electrolyzer technology	AEL	AEL	AEL	SOEC	AEL	-
FT recycle	LR	SR	SRR	LR	LR	LR
Biomass type	FR	FR	FR	FR	AR	FR

used in literature not only for PBtL [8, 35, 49] but also for BtL [50] simulations. Secondly, alkaline electrolysis has the highest technology readiness level [37]. Thirdly, average forest residue requires less effort in the syngas cleaning section [20] and is therefore the preferred option over agricultural residue.

The two other FT off-gas recycling methods, short recycle (SR) and short recycle with reformer (SRR), are discussed with the simulation cases PBtL-SR and PBtL-SRR. Further, when cases with a SOEC system are discussed instead of an AEL, these cases are denoted as PBtL-SOEC. To signify the use of agricultural residues (AR) the index notation PBtL_{AR} is used. Finally, the reference case Biomass to Liquid will be referred to with the abbreviation BtL. For all BtL simulations, a long recycle is modeled.

2.6 Techno-economic analysis

2.6.1 Technical analysis

In order to assess the process performance from a technical perspective, carbon efficiency η_C , fuel efficiency η_{Fuel} , and process efficiency $\eta_{Process}$ are considered in this study. Whereby, in all equations the product is defined as the liquid Fischer–Tropsch fraction C_{5+} . The carbon efficiency η_C , as defined in Eq. (10), shows the share of biomass' carbon atoms that can be converted to product carbon [6].

$$\eta_C = \frac{\dot{n}_{C,Prod}}{\dot{n}_{C,Biom}} \quad (10)$$

The energetic fuel efficiency is stated in Eq. (11). It shows the fraction of the input energy that can be converted to FT product. Here, the lower heating value LHV of the wet biomass and the process power requirement P_{El} are considered as energy inputs [6].

$$\eta_{Fuel} = \frac{\dot{m}_{Prod} LHV_{Prod}}{\dot{m}_{Biom} LHV_{Biom} + P_{El}} \quad (11)$$

For the process efficiency in Eq. 12, the process off-heat $\dot{Q}_{Process}$ is included as an additional product. The calculation method for process off-heat and corresponding utility integration is automated in the software tool TEPET. The underlying methodology is described in [42].

$$\eta_{Process} = \frac{\dot{m}_{Prod} LHV_{Prod} + \dot{Q}_{Process}}{\dot{m}_{Biom} LHV_{Biom} + P_{El}} \quad (12)$$

For this study, a pinch temperature of 5 °C is assumed for the heat integration. Excess heat streams at a temperature level higher than 183 °C can be used for the production of high (35.5 bar), medium (20 bar), or low (10 bar) pressure steam. Here, a brown field site is assumed, where all steam types can be sold. The cooling demand for the process is provided by cooling water with an initial temperature of 15 °C and an outlet temperature of 20 °C. Cooling below 15 °C is accomplished with a refrigeration cycle with a refrigerant temperature of -10 °C. As an example, Fig. 3 shows the composite curve after utility integration for the base case. Here, no low-pressure steam is produced. Instead, the production of 8 MW_{th} of high-pressure steam and 17 MW_{th} of medium-pressure steam is prioritized, as these pressure levels generate higher revenue. In addition, a duty of 8 MW_{th} for cooling and 0.5 MW_{th} for refrigeration is required for the process.

2.6.2 Economic analysis

The economic analysis is based on the approach published by Peters, Timmerhaus, and West [51]. The calculation algorithm implemented in DLR's techno-economic software tool TEPET is described in [6, 42]. The aim of the economic analysis is to estimate the net production costs NPC . These are calculated, according to Eq. 13, as the ratio of all production cost divided by the product mass flow [42]. Annual capital cost ACC , indirect and direct operational expenditures $OPEX$ and the hourly labor cost c_L multiplied with the number of workers per shift N_w contribute to the production cost. For all cases analyzed in this study, 7 workers per shift with hourly labor cost of 43.14 €/h [52] are assumed.

$$NPC = \frac{ACC + \sum OPEX_{ind} + \sum OPEX_{dir} + N_w c_L}{\dot{m}_{Product}} \quad (13)$$

Direct OPEX are calculated as the sum of all utility and feedstock costs and revenues for the byproducts. The corresponding utility prices can be found in Tables 3 and 6. Further, it is assumed that the plant can be operated for 8100 h per year in steady state mode, which is necessary for the economic operation especially of the electrolyzer [36]. Indirect

Fig. 3 Composite curves including heat integration for the base case. Hot streams are depicted in red, cold streams in blue. Medium pressure (MPS), high pressure steam (HPS), cooling water (CW), and refrigeration (RF) utilities are marked in the plot

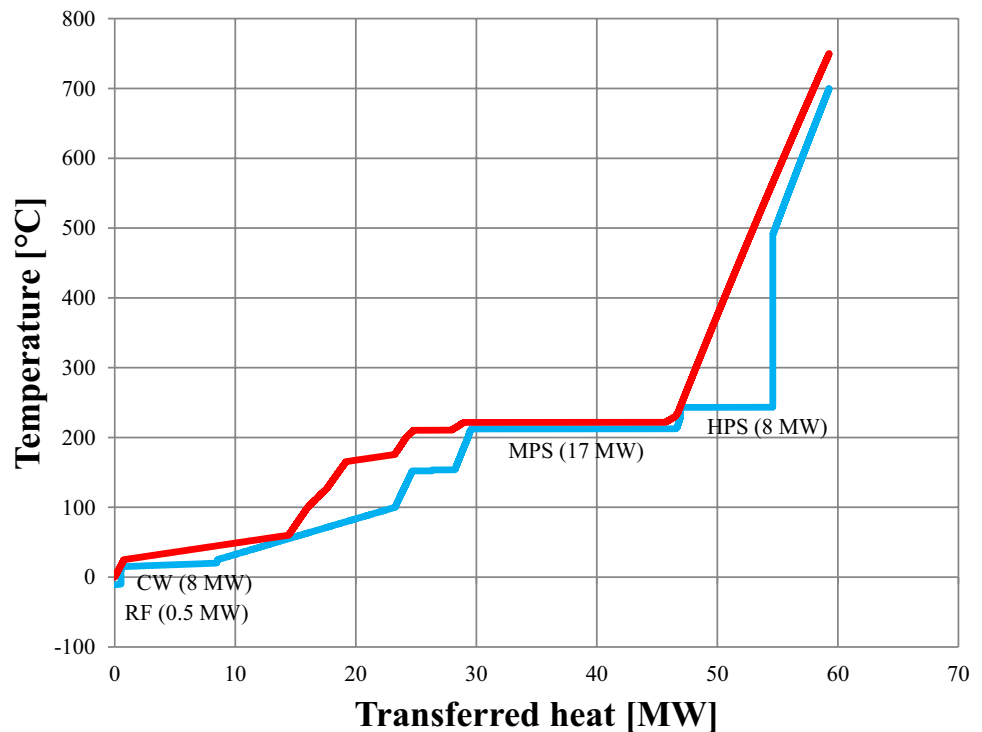


Table 3 Utility and feedstock prices used for the production cost estimation. For electricity prices, please refer to Table 6

Utility	Prices	Source
Forest residue ^a	42.23 €/t	[53]
Agricultural residue ^a	40.01 €/t	[53]
Demineralized water for electrolysis	2 €/m ³	[35]
Fresh water	0.426 €/m ³	[54]
FT catalyst ^b	33 €/kg	[55]
Gas cleaning utilities	1.437 €/t	[56]
Waste water	0.907 €/m ³	[51]
HPS	21.216 €/t	[57]
MPS	19.241 €/t	[57]
LPS	13.142 €/t	[57]
Cooling water	0.005 €/m ³	[6]

^aPrice from ENSPRESO data base for FI 2020 for the MED scenario

^bCatalyst lifetime of 5 years [58] with continuous replacement

OPEX account for additional production expenses such as maintenance, plant overhead or administration. The estimation algorithm for indirect OPEX can be taken from [6].

A plant's annual capital cost ACC is calculated according to Eq. (14). Here, the capital cost is determined by the fixed capital investment FCI , the interest rate IR , 7% for all cases, and the plant lifetime PL , for which 20 years are assumed. Fixed capital investment FCI , Eq. (15) [6], represents the equipment cost for all plant equipment E_i in combination

with their auxiliary cost, such as installation cost or cost for their instrumentation and controls. Auxiliary costs are estimated with Lang factors F_{I-12} that may vary with the analyzed equipment type, cf. Table 4. A list of all Lang factor types can be found in the Supplementary Material.

$$ACC = FCI \cdot IR \left(\frac{(1 + IR)^{PL}}{(1 + IR)^{PL} - 1} + \frac{1}{9} \right) \quad (14)$$

$$FCI = \sum_{i=1}^m E_i \left(1 + \sum_{j=1}^{10} F_{eco,i,j} \right) \left(1 + \sum_{j=11}^{12} F_{eco,i,j} \right) \quad (15)$$

$$E_i = E_{ref,i} \left(\frac{S_i}{S_{ref}} \right)^k \left(\frac{CEPCI_{2020}}{CEPCI_{ref}} \right) \quad (16)$$

The equipment costs E_i , follow from Eq. (16). Here, the cost for an equipment type is scaled up using a scaling exponent k from a reference unit, for which investment cost E_{ref} and characteristic size S_{ref} are known. The CEPCI term accounts for inflation from the reference year until 2020. A comprehensive list of all equipment cost functions can be found in Table 4.

2.7 GHG emission analysis

To assess the process' greenhouse gas (GHG) emissions, an approach focusing on the two most impactful variables,

Table 4 Equipment cost functions

Unit	E_{ref}	Currency	S_{ref}	Unit	k	Year	Source	Lang factors
Miscellaneous	3.5	M€	5.3	$\text{kg}_{\text{biom,out}}/\text{s}$	0.7	2019	[56]	E
Gas cleaning island	10.8	M€	8.25	$\text{kg}_{\text{syng,in}}/\text{s}$	0.7	2019	[56]	E
HRSG	6	M€	43.6	Transferred heat, [MW]	0.8	2010	[13]	C
ASU	13.8	M€	1.38	$\text{kg}_{\text{O}_2}/\text{s}$	0.7	2019	[56]	E
Syngas compressor	5	M€	10	Compression work, MW_e	0.67	2010	[13]	C
CO_2 compressor	5	M€	10	Compression work, MW_e	0.67	2010	[13]	C
Oxygen compressor	5.7	M€	10	Compression work, MW_e	0.67	2010	[13]	D
Gasification island ^d	31.6	M€	5.3	$\text{kg}_{\text{biom,out}}/\text{s}$	0.7	2019	[56]	E
Dryer & feedstock handling	7.5	M€	5.3	$\text{kg}_{\text{biom,out}}/\text{s}$	0.7	2019	[56]	E
Gas/liquid separator ^a	0.09	M€	10	Unit length, m	0.79	2014	[51]	A
Fischer–Tropsch SBCR ^c	2.025	M\$	341.3	Reactor volume, m^3	0.67	1998	[59]	A
AEL ^{b,c}	1	M€	1	Electrical power input, MW_e	0.8	2019	[37]	E,B
SOEC ^b	2	M€	1	Electrical power input, MW_e	1	2019	[39]	E
Reformer (short recycle)	21.8	M€	2.037	Syngas, kmol/s	0.67	2010	[13]	C
Water scrubber (short recycle)	5.2	M€	1.446	Syngas input, kmol/s	0.67	2010	[60]	3

^aCost data for storage vessels were used. The cost function has three input parameters (vessel length, vessel diameter, pressure). The stated cost function is an example based on a horizontal storage vessel with a diameter of 2 m at pressure levels up to 10 bar [6]

^bMaintenance cost 2% and 5% of stack investment for AEL and SOEC respectively [37]

^cFor exact costing method refer to [36]

^dIncludes gasifier, filter, and reformer

Table 5 Impact factors on the process GHG footprint calculation

	Value	Source
Average biomass transport radius $r_{\text{transport}}$	100 km	[18]
Biomass transport emissions $\text{GHG}_{\text{transport}}$	$69 \text{ g}_{\text{CO}_2,\text{eq}}/(\text{t km})$	[61]
RED II fossil fuel comparator	$94 \text{ g}_{\text{CO}_2,\text{eq}}/\text{MJ}$	[62]
GHG emission reduction for sustainable fuel	65%	[62]
AR harvesting $\text{GHG}_{\text{harvest}}$	$0.27 \text{ MJ}/\text{kg}_{\text{AR}}$	[63]
FR harvesting $\text{GHG}_{\text{harvest}}$	$0.21 \text{ MJ}/\text{kg}_{\text{FR}}$	[63]
Average crude oil price, Brent 2020	$41.3 \text{ \$}_{2020}/\text{bbl}$	[64]

biomass provision and electricity production [18], is taken. Assumptions for the biomass provision GHG calculation can be found in Table 5.

$$\text{GHG}_{\text{process}} = r_{\text{transport}} \text{GHG}_{\text{transport}} + \text{GHG}_{\text{harvest}} + P_{el} \text{GHG}_{el} \quad (17)$$

As shown in Eq. (17), total process emissions are calculated with transport $\text{GHG}_{\text{transport}}$, harvesting $\text{GHG}_{\text{harvest}}$ and power production emissions GHG_{el} . Whereby, harvesting and transport are powered by fossil fuel. The biomass itself is regarded as carbon-neutral.

In this study, PBtL fuel falls under the definition of transport biofuel in the RED II directive [62]. The same classification for PBtL fuel is chosen in a recent study by the Policy Department for Structural and Cohesion Policies

[65]. At the same time, the GHG emission reduction limit for sustainable fuel for 2021 is used here. Although a different limit of 60% would apply for the studied year 2020, the 65% limit is used, as plants constructed in 2020 with a lifetime of 20 years would have to be designed according to the 65% limit.

The process is analyzed with different national grid electricity mixes, whereby the Finnish grid serves as the base case. Average carbon intensity and electricity prices are listed in Table 6. For the EU grid mix, average values for all 27 member states are taken into account.

When process GHG emissions and NPC are established, the GHG abatement cost AC can be calculated with Eq. 18. The abatement costs indicate how costly the GHG savings are when using an alternative fuel instead of fossil fuel. To that end, the additional cost for producing alternative fuel ($\text{NPC}_{\text{PBtL}} - P_{\text{crude oil}}$) is divided by the amount of GHG savings expressed in CO_2 equivalents ($\text{GHG}_{\text{crude oil}} - \text{GHG}_{\text{PBtL}}$). As the price for crude oil $P_{\text{crude oil}}$ the average price for a barrel of Brent in 2020 is used. The fossil GHG emissions are calculated with the fossil fuel comparator defined in the RED II directive [68]. It should be noted that the RED II definition for fossil fuel includes the emissions during the burning process. These are not included for the alternative fuel, where only the production process has an impact on the GHG emissions. However, this assumption can be justified when considering their marginal combustion emissions [69].

Table 6 Carbon intensity and electricity price for different European grid mixes

	Average grid electricity price [€ ₂₀₂₀ /MWh] [66]*	GHG footprint electrical power GHG_{el} [kg _{CO₂,eq} /MWh] [67]
EU-27	59.3	230.7
Germany	64.3	311
Finland (base case)	45.9	68.6
Sweden	35.6	8.8
Norway	30.8	19
France	53.5	51.1

*Prices for industrial consumers > 19 MW excluding VAT and other recoverable taxes and levies

$$AC_{PBtL} = \frac{NPC_{PBtL} - P_{crudeoil}}{GHG_{crudeoil} - GHG_{PBtL}} \quad (18)$$

potential production volume (Sect. 3.5). With that, conclusions about the possible fuel provision via the PBtL process for the EU aviation sector can be derived.

3 Results and discussion

After presenting the results for the different cases defined in the Sect. 3.1, a discussion of the design options under varying economic boundary conditions can be found in Sect. 3.2. The effect of selected process parameters on the base case results is shown in Sect. 3.3 with a sensitivity analysis. Finally, BtL and PBtL base case are compared in terms of their GHG abatement cost (Sect. 3.4) and their

3.1 Techno-economic analysis

The results of the technical analysis can be taken from Table 7. The efficiency terms, as defined in Sect. 2.6.1, are displayed here along with key mass and energy flows. Similarly, economic results are shown in Table 8. For a discussion of the case studies, described in 2.5, refer to the following sections.

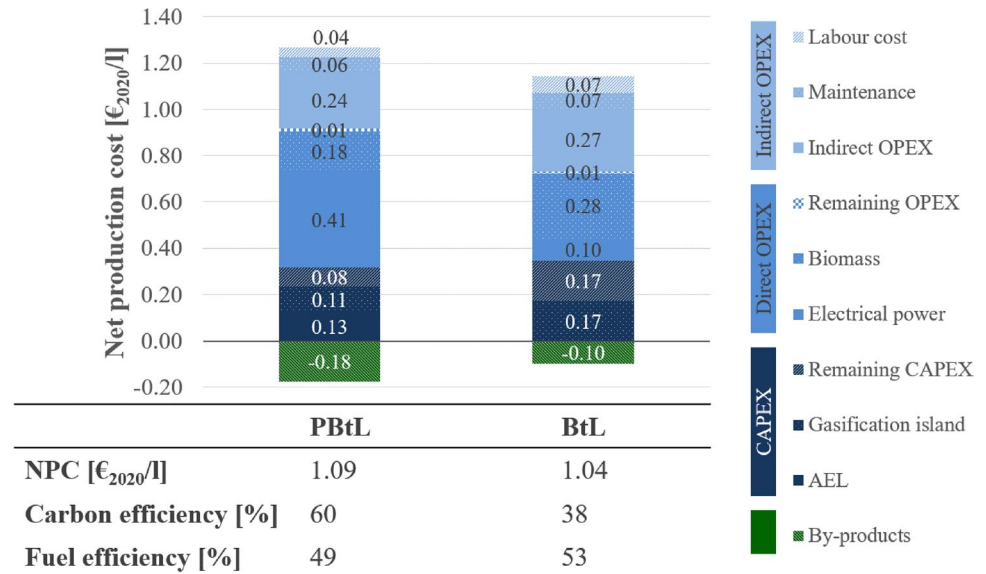
A breakdown of the NPC for the PBtL base case along with the BtL case is presented in Fig. 4. Whereby, the

Table 7 Technical analysis: selected mass and energy flows for all cases

Case		PBtL	PBtL-SR	PBtL-SRR	PBtL-SOEC	PBtL-AR	BtL
<i>Input</i>							
Wet biomass	kg/s	6.27	6.27	6.27	6.27	6.27	6.27
LHV wet biomass	MJ/kg	7.98	7.98	7.98	7.98	7.98	7.98
Total electrical power	MW _{el}	48.8	35.4	62.1	38.2	61.8	7.18
Power electrolyzer	MW _{el}	42.0	31.3	58.3	31.4	54.6	
H ₂ production	kg/s	0.21	0.16	0.29	0.21	0.27	
<i>Product</i>							
Product output	kg/s	1.098	0.621	1.259	1.098	1.105	0.689
Product LHV	MJ/kg	44.0	44.2	44.0	44.0	44.0	44.0
<i>Alkanes</i>							
C5–10	kg/s	0.204	0.155	0.239	0.204	0.207	0.129
C11–20	kg/s	0.398	0.172	0.456	0.398	0.401	0.250
C21+	kg/s	0.359	0.095	0.401	0.359	0.358	0.223
<i>Alkenes</i>							
C5+	kg/s	0.136	0.199	0.163	0.136	0.139	0.087
<i>By-products</i>							
High pressure steam	MW _{th}	7.65	6.34	8.91	4.66	15.2	7.84
Medium pressure steam	MW _{th}	17.1	15.4	21.6	10.3	15.5	0
Low pressure steam	MW _{th}	0	15.7	0	0	0	0
Process efficiency	%	73.9	75.9	76.6	71.7	71.0	66.7
Fuel efficiency	%	48.9	32.1	49.4	54.8	43.4	53.0
Carbon efficiency	%	59.8	33.8	68.5	59.8	57.4	37.5

Table 8 Economic results for all simulation cases including largest OPEX and FCI cost items

Case		PBtL	PBtL-SR	PBtL-SRR	PBtL-SOEC	PBtL _{AR}	BtL
<i>OPEX</i>	M€ ₂₀₂₀ /a						
Electricity		18.1	13.2	23.1	14.2	23	2.7
Biomass		7.8	7.8	7.8	7.8	7.3	7.8
Other		0.5	0.9	0.6	0.6	0.6	0.3
Total		26.4	21.9	31.5	22.6	30.9	10.8
<i>Revenue by-product</i>	M€ ₂₀₂₀ /a	7.7	9.7	9.5	4.7	9.9	2.7
<i>FCI</i>	M€ ₂₀₂₀						
Electrolyzer		53.9	41.1	72.9	60.4	68.7	0
Gasification island		46.2	46.2	46.2	46.2	46.2	46.2
Fischer–Tropsch reactor		11.7	38.2	13.7	11.7	11.9	8.3
Gas cleaning island		13.6	9.5	9.5	13.6	15.1	12.3
Recycle reformer		0	0	14	0	0	0
Other		10.6	6.9	11	10.6	11.7	26.2
Total		135.9	141.9	167.3	142.5	153.5	92.9
<i>Indirect OPEX</i>	M€ ₂₀₂₀ /a	10.6	10.9	12.2	10.9	11.5	8.4
NPC	€ ₂₀₂₀ /l	1.09	1.68	1.13	1.10	1.21	1.04

Fig. 4 Comparison of PBtL and BtL base case including the breakdown of NPC in €₂₀₂₀/l by cost type

liquid FT product fraction has a density of 0.729 kg/l. Given the analyzed economic boundary conditions, production costs for PBtL are 0.05 €₂₀₂₀/l higher. Hereby, the largest NPC drivers for PBtL are the feedstock cost, electricity and biomass, and the electrolyzer investment cost.

Additionally, Fig. 4 shows carbon and fuel efficiency for both process types. Although the fuel efficiency is rather similar for BtL and PBtL, a large difference in carbon efficiency can be found. The higher carbon efficiency follows from the higher product output based on the same biomass input, which can be attributed to the CO₂ recycle. Yet, the recycle necessitates the electrolyzer to adjust the H₂/CO ratio in the syngas to the stoichiometric value of 2.1. The

effects of an increased CO₂ recycling rate on NPC and carbon efficiency are further discussed in Sect. 3.2.

3.2 Discussion of design options under varying boundary conditions

The technical and economic results for the process design options under Finnish boundary conditions are presented in Sect. 3.1. To highlight the advantages of certain process design options, those are discussed under varying economic boundary conditions.

3.2.1 Electrolyzer choice and CO₂ recycling under variable electricity price

The electricity cost is the largest operation cost contributor to the PBtL process under Finnish conditions, as seen in Table 8. In Fig. 5, the electricity price is varied for BtL as well as PBtL with the two electrolyzer options, AEL and SOEC. Changing electricity prices have the largest effect on the PBtL-AEL NPC. This is due to the large power demand for the AEL compared to the other cases, as shown in Table 7.

Overall, the base case PBtL-AEL has the economic edge over BtL and PBtL-SOEC at electricity prices lower than 39.4 €/MWh. At higher prices, the BtL process is the preferable option. The advantage of the SOEC, its higher electrolytic efficiency, gains importance at higher electricity prices. Yet, the lower investment cost for the AEL system makes it the more cost effective technology choice at low electricity prices.

For the cases analyzed thus far, the CO₂ recycling is iterated to attain an oxygen dilution rate of 65% in the gasifier feed (cf. Section 2.4.2). This amounts to a CO₂ recycling ratio of 44% for the base case. In Fig. 6, the effect of

changing the CO₂ recycle rate is depicted. Here, the oxygen dilution is varied from 10 to 100% resulting in a CO₂ recycle rate of 7 to 70%.

As can be taken from the left plot in Fig. 6, the carbon efficiency and thereby the product yield of the process increases with the CO₂ recycling rate. This is to be expected, as more biogenic carbon leaves the gasification island as CO. Yet, the increased CO output leads to a reduction in the syngas' H₂/CO ratio. In the analyzed CO₂ recycle range, the H₂/CO ratio drops from 2.05 to 1.34. Subsequently, more electrical power is needed to adjust the H₂/CO ratio to the stoichiometric value of 2.1. At the maximum CO₂ recycling rate, 80 MW_{el} total energy input are required while only 8 MW_{el} are needed for the minimal rate.

The right plot in Fig. 6 shows which effect a higher CO₂ recycling rate has on the NPC when assuming different electricity prices. For the Finnish electricity price in 2020 (45.9 €/MWh), increased recycling leads to higher NPC. Here, the additional electricity costs outweigh the cost benefits of a higher product output. Only for electricity prices lower than 20 €/MWh, a decrease in NPC can be expected. This parameter variation shows an example, how the optimal plant configuration is influenced by the local cost boundary

Fig. 5 NPC over electricity price for the base case PBtL-AEL (dark blue), PBtL-SOEC (light blue), and BtL (green)

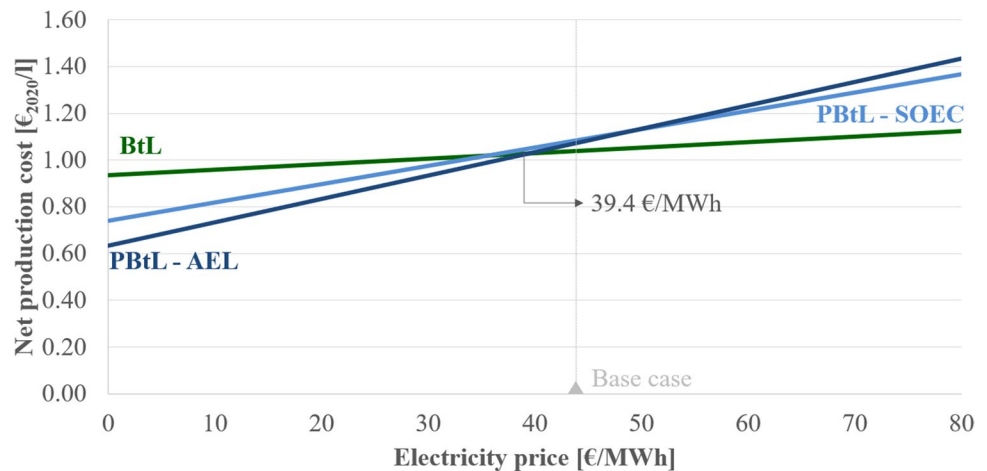
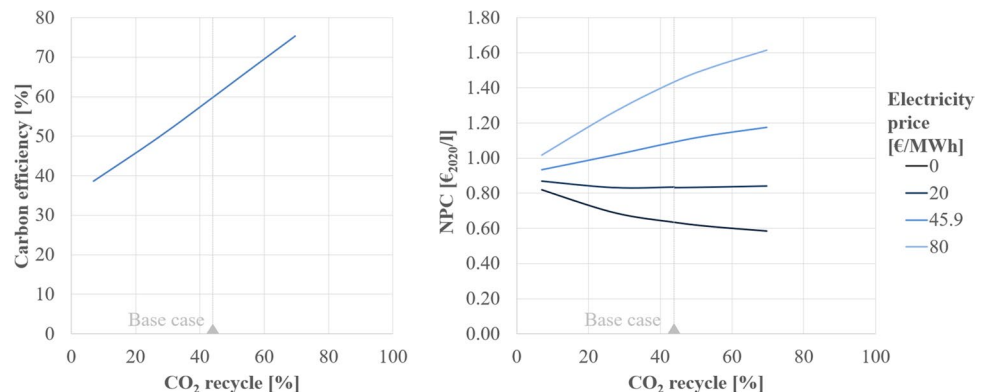


Fig. 6 Effect of an increase in CO₂ recycle rate on carbon efficiency (left) and NPC (right) for the PBtL base case



conditions. An optimal CO₂ recycling rate can only be determined with a techno-economic assessment.

3.2.2 Recycle options and feedstock

Figure 7 compares NPC for the analyzed recycle options when using forest residue (FR) or agricultural residue (AR) as feedstock. It is apparent that for both biomass types SR results in the highest NPC: 1.68 €₂₀₂₀/l for FR and 2.16 €₂₀₂₀/l for AR. This suggests that reforming the recycled FT gas fraction C₁₋₄ is economically reasonable under the given economic constraints. As the SR option has the lowest power demand of all PBtL recycle options (cf. Table 7), an argument can be made for using the SR at high electricity prices.

A slight NPC advantage can be found for the LR over the SRR option for forest residue. Here, the base case PBtL_{FR}-LR (1.09 €₂₀₂₀/l) has lower NPC than PBtL_{FR}-SRR (1.13 €₂₀₂₀/l). Yet, the advantage is reversed when using agricultural residue, with 1.21 €₂₀₂₀/l for PBtL_{AR}-LR against 1.20 €₂₀₂₀/l for PBtL_{AR}-SRR. As shown in Table 7, a higher product yield is found for the SRR case which comes at the cost of a higher electrolysis power input. This results in

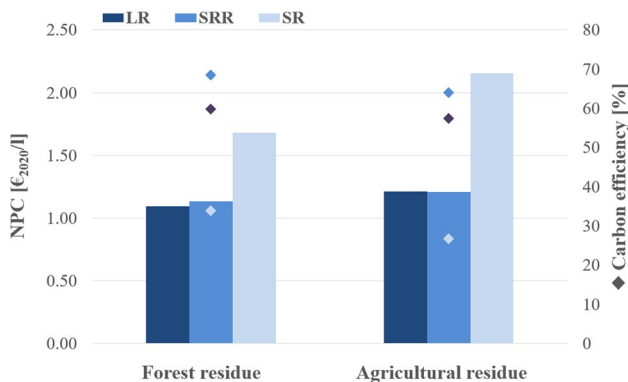


Fig. 7 NPC shown with bars for short (SR), long (LR), and short recycle with reformer (SRR) using forest residue or agricultural residue. The carbon efficiency for all design options is indicated with diamond shapes referring to the right axis

lower NPC for the LR case with FR at the base case electricity prices of 45.9 €₂₀₂₀/MWh. When using agricultural residue as feedstock, the filter temperature is decreased and reformer temperature increased compared to the forest residue case. This results in a higher electrolytic hydrogen demand. Therefore, a cost advantage can be found for the SRR option because the reformer recycle can be avoided. Overall, both options, SRR and LR, can be favorable options depending on the economic boundary conditions and should both be considered when designing a PBtL process.

The forest residue cases in Fig. 7 show consistently lower NPC and higher carbon efficiencies. This is due to the less intensive syngas treatment for forest residue. The lower tar formation rate allows for a syngas treatment with higher filter and lower reformer temperature compared to agricultural residues.

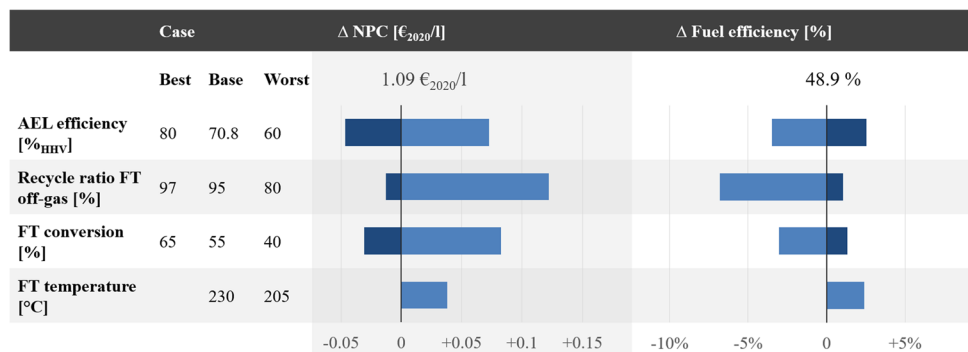
3.3 Base case sensitivity analysis

The effects of selected process parameters on NPC, carbon and fuel efficiency for the PBtL base case are displayed in Fig. 8. Here, the four parameters electrolyzer efficiency, recycle ratio, FT conversion, and temperature were chosen for their impact and uncertainty underlying their base case assumption.

The alkaline electrolyzer efficiency is simulated in the base case with a system efficiency of 70.8%_{HHV}. In an expert elicitation study, Schmidt et al. [39] display system efficiency predictions that go as high as 80%_{HHV}. Those predictions are connected to further development of the zero-gap AEL technology [70]. As a worst-case assumption, a system efficiency of 60%_{HHV} is used.

The FT off-gas recycle rate is set to 95% in the base case. Although a higher recycling rate leads to increased overall syngas conversion, it is unclear how much off-gas can be recycled to the reformer. Inert gas components, such as N₂ formed in the gasifier, will accumulate in the recycle loop. Correspondingly, full recirculation is not possible. As a best-case assumption 97% is chosen. The worst-case is simulated with an 80% recycle.

Fig. 8 Sensitivity of NPC and process efficiency to process parameters varied in the PBtL base case. Result for best (dark blue) and worst (light blue) case given as the absolute difference to the base case results



To avoid the deactivation of the FT catalyst, the CO conversion should be limited [34]. Rytter and Holmen report a conversion limit of 65% for a slurry-bubble column reactor using cobalt catalyst [34]. Along with the base case assumption of 55% CO conversion [8], a worst-case of 40% is analyzed.

For low-temperature catalyst, the Fischer–Tropsch reactor operation temperature is typically given in the range of 190–240 °C [5]. The used reaction kinetic is based on experimental data in the range of 205–230 °C [46]. Therefore, worst and base case FT temperatures are chosen according to [46] as 205 °C and 230 °C.

Overall, a correlation of fuel efficiency and NPC can be observed in Fig. 8. Except for the FT temperature, higher fuel efficiency leads to lower NPC. This underlines the significance of low OPEX for the PBtL process. Higher NPC at low FT temperatures result from an increased capital expenditure for the FT reactor. Due to the lowered catalyst activity at 205 °C, more catalyst is needed to attain the same CO conversion. The higher product yield, a result of the higher product selectivity at low FT temperatures, cannot compensate for the higher FT reactor investment.

3.4 GHG abatement cost

The resulting fuel emissions, calculated according to the methodology described in Sect. 2.7, can be taken from the bar chart in Fig. 9. Here, it is assumed that the PBtL base case (blue) and the BtL reference case (green) are operated with different European national grid mixes. From fuel production emissions and NPC, the nation-specific abatement

costs can be calculated, which are depicted with diamond shapes referring to the right y-axis.

Using the PBtL base case configuration, only countries with low GHG footprint in their national grid can produce fuel that can be counted as sustainable according to the RED II directive in 2020 [62]. Here, a 65% reduction compared to fossil fuel has to be met for the sustainability limit, i.e., 32.9 g_{CO₂,eq}/MJ. Using the German and EU-27 average electricity grid mix, this limit is exceeded. To stay under the limit, the electricity GHG footprint should not be higher than 116 kg_{CO₂,eq}/MWh. All BtL cases, on the other hand, meet the sustainability limit due to their lower electricity demand.

Abatement costs scale with the electricity price and the electricity's GHG footprint. For this reason, PBtL abatement costs for EU-27 and Germany are higher than 1000 €/t_{CO₂,eq}, while Finland, Sweden, France, and Norway lie below 420 €/t_{CO₂,eq}. As considerably less electricity is needed for the BtL process, GHG abatement cost range from 300 to 430 €/t_{CO₂,eq} for the selected examples. Only for countries with relatively low electricity price and GHG footprint, such as Sweden or Norway, the PBtL GHG abatement costs lie below BtL. This underlines the importance of green and inexpensive electricity for the PBtL process.

3.5 EU fuel potential analysis

Figure 10 shows the potential product output, if all currently available EU forest and agricultural residue is converted to fuel via the PBtL or the BtL route. The calculation is based on a total availability of 40 Mt_{dry}/a forestry and 139 Mt_{dry}/a agricultural residue in the EU [31]. The presented

Fig. 9 Specific fuel production emissions indicated by bars and GHG abatement costs (AC) indicated by diamond shapes for the PBtL base case (blue) and BtL (green) using different national electricity grid mixes

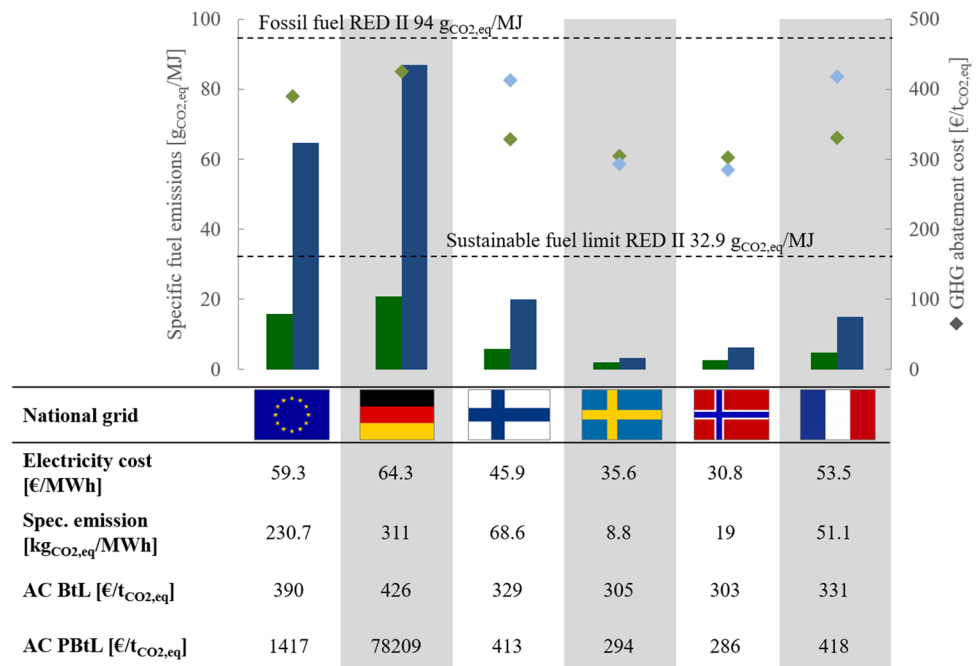
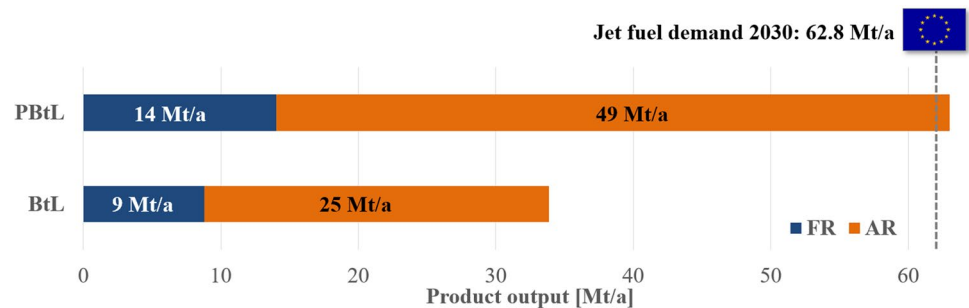


Fig. 10 Fuel production potential in the EU using forest residue (blue) and agricultural residue (orange) for BtL and PBtL (base case)



absolute product output values should be taken as an optimistic approximation. For one, only a part of the product fraction C_{5+} could actually be converted to SAF. Secondly, for a more exact estimation, local production conditions would have to be considered with locally varying biomass compositions and availability, as other sectors, such as heat and power production, compete for biomass residue as their feedstock. Still, the calculation allows for a comparison of BtL and PBtL because these optimistic assumptions affect both processes equally.

With the given assumptions, PBtL could produce around double the output (63 Mt/a) compared to BtL (34 Mt/a), whereby the agricultural residue makes up the bulk (~75%) of feedstock. The EU's jet fuel demand in 2030 of 62.8 Mt/a [7] could be met with PBtL when full biomass utilization is assumed. Yet, for this product output an installed AEL capacity of 101 GW_{el} or 14.8 Mt/a of hydrogen would be required. Given that the European Commission only aims for a total H₂ production rate of 10 Mt/a by 2030 [71], a substantial contribution the SAF production by the PBtL process can only be expected in later decades. Nevertheless, the results highlight the PBtL advantage over the BtL process of having a higher conversion rate of the limited biomass residue feedstock. This advantage could even be extended further with an increased CO₂ recycling rate. Yet, the greater yield would have to be weight against the additional hydrogen demand as described in Sect. 3.2.1.

4 Conclusions

The Power and Biomass to Liquid (PBtL) process presents a promising pathway for the production of low GHG fuel. In this study, a techno-economic and GHG emission analysis has been conducted for a small-scale PBtL plant with a biomass input of 50 MW_{th} and a 42 MW_{el} alkaline electrolyzer producing 32 kt/a Fischer–Tropsch product. The analysis has been conducted on the basis of an Aspen Plus process model relying on experimental data from the EU project FLEXCHX as well as unit models from literature. Different process design options and a comparative Biomass to Liquid (BtL) case were assessed under varying economic boundary

conditions. Based on the findings in this study, the following assertions can be made:

- For the PBtL base case, net production costs (NPC) of 1.09 €₂₀₂₀/l have been estimated. Thereby, the cost for electrical power, biomass, and the AEL investment constitute the largest contributions to OPEX and CAPEX.
- The optimal process design and even the choice to use electrolytic hydrogen, largely depend on the local boundary conditions. A techno-economic analysis provides a good indication, which option to favor, but needs to be confirmed during the detailed design phase of any pursued project: The short recycle reformer (SRR) is advantageous at low electricity prices and when using feedstock requiring a high gas-cleaning effort. Short recycling (SR) should be avoided, if long recycle (LR) or SRR are feasible.
- Favoring an SOEC over an AEL electrolyzer is economically reasonable at high electricity prices. Here, the higher system efficiency can make up for the SOEC's higher investment costs.
- CO₂ recycling increases the carbon efficiency and, thereby, the product output. However, more hydrogen is required for the conversion. Therefore, NPC only fall with higher CO₂ recycling rates, if the electricity price is below a certain threshold. For the base case, the price threshold is around 20 €₂₀₂₀/MWh.
- Generalizing from the two exemplary feedstocks analyzed in this study, it can be concluded that forest residue (FR) has a higher fuel efficiency and lower NPC than agricultural residue (AR). This is due to the on average lower tar formation rate for FR. Yet, in the EU more AR is available. The potential EU fuel output could be increased three-fold when utilizing AR in addition to FR.
- At low electricity prices (< 39.4 €/MWh), PBtL is the more cost-effective process option in comparison to BtL. In addition, a higher product output at similar fuel and process efficiencies can be expected. When converting the entire EU AR and FR potential, around double the fuel output would be generated with PBtL.
- Low GHG electricity is needed to produce sustainable fuel in accordance with the RED II directive: With the

German average 2020 grid mix of 311 g_{CO₂,eq}/MJ the RED II threshold of 32.9 g_{CO₂,eq}/MJ could not be met. For the base case, the electricity GHG footprint should not be higher than 116 kg_{CO₂,eq}/MWh. This is the case for countries like France, Finland, Sweden or Norway.

- For low GHG abatement costs green and inexpensive electricity is required: With the Norwegian or Swedish grid mix PBtL abatement costs below those of BtL can be reached.

The availability of green and inexpensive electricity is necessary for the production of fuel via the PBtL process. These conditions are not met in many countries in Europe. However, governments and industry are working on the reduction of GHG emissions from their national power production. In the opinion of the authors, fuel production in these countries should be ramped-up via the BtL process while this transition is under way. At a later stage, the process can be converted to PBtL by the addition of an electrolysis unit. This will increase the conversion of limited biomass residue.

Supplementary information The online version contains supplementary material available at <https://doi.org/10.1007/s13399-022-03671-y>.

Acknowledgements The authors would like to gratefully acknowledge the funding provided by the European Union's Horizon 2020 research and innovation program under Grant Agreement No 763919. Further, the authors would like to thank Julia Weyand, Moritz Raab, and for their valuable inputs.

Author contribution The study is based on Esa Kurkela process design as studied in the EU project FLEXCHX. Modeling, simulation, and analysis were done by Felix Habermeyer under the guidance of Ralph-Uwe Dietrich and Esa Kurkela. The GHG emission analysis was conducted by Julia Weyand. The software tool TEPET was provided by Simon Maier. The author Felix Habermeyer prepared the manuscript. Ralph-Uwe Dietrich, Esa Kurkela, Julia Weyand, and Simon Maier discussed and commented the manuscript.

Funding Open Access funding enabled and organized by Projekt DEAL. This study is part of the FLEXCHX project, which has received funding from the European Union's Horizon 2020 research and innovation Programme under Grant Agreement No 763919.

Data availability All data and materials as well as software application or custom code comply with field standards. Additional data is available in the Supporting Material.

Declarations

Ethical approval Not applicable.

Conflict of interest The authors declare no competing interests.

Open Access This article is licensed under a Creative Commons Attribution 4.0 International License, which permits use, sharing, adaptation, distribution and reproduction in any medium or format, as long as you give appropriate credit to the original author(s) and the source, provide a link to the Creative Commons licence, and indicate if changes

were made. The images or other third party material in this article are included in the article's Creative Commons licence, unless indicated otherwise in a credit line to the material. If material is not included in the article's Creative Commons licence and your intended use is not permitted by statutory regulation or exceeds the permitted use, you will need to obtain permission directly from the copyright holder. To view a copy of this licence, visit <http://creativecommons.org/licenses/by/4.0/>.

References

1. European Commission (2019) The European green deal. https://eur-lex.europa.eu/resource.html?uri=cellar:b828d165-1c22-11ea-8c1f-01aa75ed71a1.0002.02/DOC_1&format=PDF. Accessed 17 Jan 2023
2. European Commission (2021) Proposal for a regulation of the European parliament and of the council on ensuring a level playing field for sustainable air transport. https://ec.europa.eu/info/sites/default/files/refuelev_aviation_-_sustainable_aviation_fuels.pdf. Accessed 17 Jan 2023
3. The White House (2021) Biden administration advances the future of sustainable fuels in American aviation. <https://www.whitehouse.gov/briefing-room/statements-releases/2021/09/09/fact-sheet-biden-administration-advances-the-future-of-sustainable-fuels-in-american-aviation/#:~:text=Current%20levels%20of%20domestic%20SAF,driving%20domestic%20innovation%20and%20deployment>. Accessed 17 Jan 2023
4. Shahriar MF, Khanal A (2022) The current techno-economic, environmental, policy status and perspectives of sustainable aviation fuel (SAF). *Fuel* 325. <https://doi.org/10.1016/j.fuel.2022.124905>
5. Ail SS, Dasappa S (2016) Biomass to liquid transportation fuel via Fischer Tropsch synthesis—technology review and current scenario. *Renew Sust Energy Rev* 58:267–286
6. Albrecht FG, König DH, Baucks N, Dietrich R-U (2017) A standardized methodology for the techno-economic evaluation of alternative fuels—a case study. *Fuel* 194:511–526. <https://doi.org/10.1016/j.fuel.2016.12.003>
7. O'malley J, Pavlenko N, Searle S (2021) Estimating sustainable aviation fuel feedstock availability to meet growing European Union demand. International Council on Clean Transportation. <https://theicct.org/publication/estimating-sustainable-aviation-fuel-feedstock-availability-to-meet-growing-european-union-demand/>. Accessed 17 Jan 2023
8. Hillestad M, Ostadi M, Serrano GA, Rytter E, Austbø B, Pharoah J, Burheim OS (2018) Improving carbon efficiency and profitability of the biomass to liquid process with hydrogen from renewable power. *Fuel* 234:1431–1451
9. Isaacs SA, Staples MD, Allroggen F, Mallapragada DS, Falter CP, Barrett SR (2021) Environmental and economic performance of hybrid power-to-liquid and biomass-to-liquid fuel production in the United States. *Environ Sci Technol* 55:8247–8257
10. Nielsen AS, Ostadi M, Austbø B, Hillestad M, del Alamo G, Burheim O (2022) Enhancing the efficiency of power-and biomass-to-liquid fuel processes using fuel-assisted solid oxide electrolysis cells. *Fuel* 321:123987
11. Dossow M, Dieterich V, Hanel A, Spliethoff H, Fendt S (2021) Improving carbon efficiency for an advanced biomass-to-liquid process using hydrogen and oxygen from electrolysis. *Renew Sustain Energy Rev* 152:111670
12. Clausen LR (2017) Energy efficient thermochemical conversion of very wet biomass to biofuels by integration of steam drying, steam electrolysis and gasification. *Energy* 125:327–336

13. Hannula I (2016) Hydrogen enhancement potential of synthetic biofuels manufacture in the European context: a techno-economic assessment. *Energy* 104:199–212. <https://doi.org/10.1016/j.energy.2016.03.119>
14. Menin L, Benedetti V, Patuzzi F, Baratieri M (2020) Techno-economic modeling of an integrated biomethane-biomethanol production process via biomass gasification, electrolysis, biomethanation, and catalytic methanol synthesis. *Biomass Conversion and Biorefinery* 13:1–22. <https://doi.org/10.1007/s13399-020-01178-y>
15. Poluzzi A, Guandalini G, Guffanti S, Elsidio C, Moiola S, Huttenhuis P, Rexwinkel G, Martelli E, Groppi G, Romano MC (2022) Flexible power & biomass-to-methanol plants: design optimization and economic viability of the electrolysis integration. *Fuel* 310:122113
16. Zhang H, Wang L, Maréchal F, Desideri U (2020) Techno-economic evaluation of biomass-to-fuels with solid-oxide electrolyzer. *Appl Energy* 270:115113
17. Bernical Q, Joulia X, Noirot-Le Borgne I, Floquet P, Baurens P, Boissonnet G (2013) Sustainability assessment of an integrated high temperature steam electrolysis-enhanced biomass to liquid fuel process. *Ind Eng Chem Res* 52:7189–7195
18. Koponen K, Hannula I (2017) GHG emission balances and prospects of hydrogen enhanced synthetic biofuels from solid biomass in the European context. *Appl Energy* 200:106–118
19. Kurkela E, Kurkela M, Frilund C, Hiltunen I, Rollins B, Steele A (2021) Flexible hybrid process for combined production of heat, power and renewable feedstock for refineries. *Johnson Matthey Technology Review* 65:333–345. <https://doi.org/10.1595/205651321X16013744201583>
20. Kurkela E, Kurkela M, Hiltunen I (2021) Pilot-scale development of pressurized fixed-bed gasification for synthesis gas production from biomass residues. *Biomass Conversion and Biorefinery* 1–22. <https://doi.org/10.1007/s13399-021-01554-2>
21. Frilund C, Tuomi S, Kurkela E, Simell P (2021) Small- to medium-scale deep syngas purification: Biomass-to-liquids multi-contaminant removal demonstration. *Biomass Bioenergy* 148:106031. <https://doi.org/10.1016/j.biombioe.2021.106031>
22. Müller S, Groß P, Rauch R, Zweiler R, Aichernig C, Fuchs M, Hofbauer H (2018) Production of diesel from biomass and wind power–energy storage by the use of the Fischer-Tropsch process. *Biomass Convers Biorefinery* 8:275–282
23. Shell Global (2021) Shell starts up Europe's largest PEM green hydrogen electrolyser. <https://www.shell.com/media/news-and-media-releases/2021/shell-starts-up-europes-largest-pem-green-hydrogen-electrolyser.html>. Accessed 18 Aug 2021
24. Violidakis I, Drosatos P, Nikolopoulos N (2017) Critical review of current industrial scale lignite drying technologies. *Low-Rank Coals for Power Generation, Fuel Chemical Production* 41–71. <https://doi.org/10.1016/B978-0-08-100895-9.00003-6>
25. Peduzzi E, Boissonnet G, Haarlemmer G, Maréchal F (2018) Thermo-economic analysis and multi-objective optimisation of lignocellulosic biomass conversion to Fischer-Tropsch fuels. *Sustain Energy Fuels* 2:1069–1084
26. Bajirao UR (2012) Kinetics and reaction engineering aspects of syngas production by the heterogeneously catalysed reverse water gas shift reaction. Dissertation, Universität Bayreuth
27. Sikarwar VS, Zhao M, Fennell PS, Shah N, Anthony EJ (2017) Progress in biofuel production from gasification. *Prog Energy Combust Sci* 61:189–248. <https://doi.org/10.1016/j.pecs.2017.04.001>
28. Van Der Laan GP, Beenackers AACM (1999) Kinetics and selectivity of the Fischer-Tropsch synthesis: a literature review. *Catal Rev* 41:255–318
29. LeViness S (2013) Velocys Fischer-Tropsch synthesis technology—comparison to conventional FT technologies. In: AIChE 2013 Spring Meeting, San Antonio, Texas
30. Jeswani HK, Chilvers A, Azapagic A (2020) Environmental sustainability of biofuels: a review. *Proc Math Phys Eng Sci* 476:20200351. <https://doi.org/10.1098/rspa.2020.0351>
31. MMalins C, Searle S, Baral A, Turley D, Hopwood L (2014) Wasted: Europe's untapped resource: an assessment of advanced biofuels from wastes and residues. International Council on Clean Transportation. <https://theicct.org/wp-content/uploads/2021/06/WASTED-final.pdf>. Accessed 17 Jan 2023
32. Searle SY, Malins CJ (2016) Waste and residue availability for advanced biofuel production in EU Member States. *Biomass Bioenergy* 89:2–10. <https://doi.org/10.1016/j.biombioe.2016.01.008>
33. Panoutsou C, Maniatis K (2021) Sustainable biomass availability in the EU, to 2050. Concawe. https://www.fuelseurope.eu/uploads/files/modules/publications/1661417357_Sustainable-Biomass-Availability-in-the-EU-Part-I-and-II-final-version.pdf. Accessed 17 Jan 2023
34. Rytter E, Holmen A (2017) Perspectives on the effect of water in cobalt Fischer-Tropsch synthesis. *ACS Catal* 7:5321–5328
35. Albrecht FG, Dietrich R-U (2018) Technical and economic optimization of Biomass-to-Liquid processes using exergoeconomic analysis. In: 26th European Biomass Conference & Exhibition (EUBCE), Copenhagen
36. Habermeyer F, Kurkela E, Maier S, Dietrich R-U (2021) Techno-economic analysis of a flexible process concept for the production of transport fuels and heat from biomass and renewable electricity. *Frontiers in Energy Research* 9:684. <https://doi.org/10.3389/fenrg.2021.723774>
37. Buttler A, Spliethoff H (2018) Current status of water electrolysis for energy storage, grid balancing and sector coupling via power-to-gas and power-to-liquids: a review. *Renew Sustain Energy Rev* 82:2440–2454
38. AsahiKasei (2020) <https://www.asahi-kasei.com/news/2020/ze200403.html>. Accessed 10 Aug 2021
39. Schmidt O, Gambhir A, Staffell I, Hawkes A, Nelson J, Few S (2017) Future cost and performance of water electrolysis: an expert elicitation study. *Int J Hydrogen Energy* 42:30470–30492. <https://doi.org/10.1016/j.ijhydene.2017.10.045>
40. Gao X, Zhang Y, Li B, Zhao Y, Jiang B (2016) Determination of the intrinsic reactivities for carbon dioxide gasification of rice husk chars through using random pore model. *Bioresour Technol* 218:1073–1081. <https://doi.org/10.1016/j.biortech.2016.07.057>
41. Smith A, Klosek J (2001) A review of air separation technologies and their integration with energy conversion processes. *Fuel Process Technol* 70:115–134
42. Maier S, Tuomi S, Kihlman J, Kurkela E, Dietrich R-U (2021) Techno-economically-driven identification of ideal plant configurations for a new biomass-to-liquid process – A case study for Central-Europe. *Energ Conver Manage* 247:114651. <https://doi.org/10.1016/j.enconman.2021.114651>
43. Aspen Technology Inc. (2013) Aspen physical property system - physical property methods. <https://docplayer.net/51476064-Aspen-physical-property-system-physical-property-models.html>. Accessed 17 Jan 2023
44. Adelung S (2022) Global sensitivity and uncertainty analysis of a Fischer-Tropsch based power-to-liquid process. *J CO2 Utilization* 65:102171
45. VTT (2020) Design and performance report for the reformer and final gas cleaning. Confidential FLEXCHX deliverable report D4.3
46. Todici B, Ma W, Jacobs G, Nikacevic N, Davis BH, Bukur D (2017) Kinetic modeling of secondary methane formation and

- 1-olefin hydrogenation in Fischer-Tropsch synthesis over a cobalt catalyst. *Int J Chem Kinet* 49:859–874
47. Todici B, Ma W, Jacobs G, Davis BH, Bukur DB (2014) CO-insertion mechanism based kinetic model of the Fischer-Tropsch synthesis reaction over Re-promoted Co catalyst. *Catal Today* 228:32–39. <https://doi.org/10.1016/j.cattod.2013.08.008>
 48. Todici B, Bhatelia T, Froment GF, Ma W, Jacobs G, Davis BH, Bukur DB (2013) Kinetic model of Fischer-Tropsch synthesis in a slurry reactor on Co-Re/Al₂O₃ catalyst. *Ind Eng Chem Res* 52:669–679
 49. Ostadi M, Rytter E, Hillestad M (2019) Boosting carbon efficiency of the biomass to liquid process with hydrogen from power: the effect of H₂/CO ratio to the Fischer-Tropsch reactors on the production and power consumption. *Biomass Bioenerg* 127:105282. <https://doi.org/10.1016/j.biombioe.2019.105282>
 50. Haarlemmer G, Boissonnet G, Imbach J, Setier P-A, Peduzzi E (2012) Second generation BtL type biofuels – a production cost analysis. *Energ Environ Sci* 5:8445. <https://doi.org/10.1039/C2EE21750C>
 51. Peters MS, Timmerhaus KD, West RE, Timmerhaus K, West R (1968) Plant design and economics for chemical engineers. McGraw-Hill, New York
 52. Krebs S (2015) Arbeitskosten pro Stunde im Verarbeitenden Gewerbe (2015). Volkswirtschaft und Statistik, VDMA. <https://www.vdma.org/documents/105628/778064/Internationaler%20Arbeitskostenvergleich%20Verarbeitendes%20Gewerbe/05a1a0bf-ea29-4a7a-b905-37ffec17957>. Accessed 16 Nov 2020
 53. Ruiz P, Nijs W, Tarvydas D, Sgobbi A, Zucker A, Pilli R, Jonsson R, Camia A, Thiel C, Hoyer-Klick C (2019) ENSPRESO—an open, EU-28 wide, transparent and coherent database of wind, solar and biomass energy potentials. *Energ Strat Rev* 26:100379
 54. Kempegowda RS, del Alamo G, Berstad D, Bugge M, Matas Güell B, Tran K-Q (2015) CHP-integrated fischer-tropsch biocrude production under norwegian conditions: techno-economic analysis. *Energy Fuels* 29:808–822
 55. Swanson RM, Platon A, Satrio JA, Brown RC (2010) Techno-economic analysis of biomass-to-liquids production based on gasification. *Fuel* 89:S11–S19
 56. VTT (2020) Gasification process design and performance report. Confidential FLEXCHX deliverable report D3.3.
 57. Eurostat (2016) Gas prices for industrial consumers. https://ec.europa.eu/eurostat/web/products-datasets/-/NRG_PC_203. Accessed 17 Jan 2023
 58. De Klerk A (2012) Fischer-tropsch refining. John Wiley & Sons
 59. Bechtel (1998) Aspen process flowsheet simulation model of a battelle biomass-based gasification, Fischer–Tropsch liquefaction and combined-cycle power plant. US Department of Energy (DOE) Pittsburgh, Pennsylvania. <https://www.osti.gov/servlets/purl/1395>. Accessed 17 Jan 2023
 60. Hannula I (2015) Co-production of synthetic fuels and district heat from biomass residues, carbon dioxide and electricity: performance and cost analysis. *Biomass Bioenerg* 74:26–46
 61. NTM (2021) Road cargo transport baselines Europe. <https://www.transportmeasures.org/en/wiki/evaluation-transport-suppliers/road-transport-baselines-2020/>. Accessed 10 June 2022
 62. European Parliament Council of the European Union (2018) Directive (EU) 2018/2001 of the European Parliament and of the Council of 11 December 2018 on the promotion of the use of energy from renewable sources. <http://data.europa.eu/eli/dir/2018/2001/oj>. Accessed 17 Jan 2023
 63. Karlsson H, Börjesson P, Hansson P-A, Ahlgren S (2014) Ethanol production in biorefineries using lignocellulosic feedstock—GHG performance, energy balance and implications of life cycle calculation methodology. *J Clean Prod* 83:420–427
 64. Index Mundi (2022) Crude oil (petroleum) monthly price - US dollars per barrel. <https://www.indexmundi.com/commodities/?commodity=crude-oil&months=60>. Accessed 10 Jun 2022
 65. Gerard F, Gorner M, Lemoine P, Moerenhout J, De Haas V, Cazola P (2022) Assessment of the potential of sustainable fuels in transport in the context of the Ukraine/Russia crisis. [https://www.europarl.europa.eu/RegData/etudes/IDAN/2022/699650/IPOL_IDA\(2022\)699650_EN.pdf](https://www.europarl.europa.eu/RegData/etudes/IDAN/2022/699650/IPOL_IDA(2022)699650_EN.pdf). Accessed 17 Jan 2023
 66. Eurostat (2021) Electricity prices for non-household consumers - bi-annual data. <http://appsso.eurostat.ec.europa.eu/nui/submitViewTableAction.do>. Accessed 31 Jan 2022
 67. Agency EE (2022) Greenhouse gas emission intensity of electricity generation by country https://www.eea.europa.eu/data-and-maps/daviz/co2-emission-intensity-9/#tab-googlechartid_googlechartid_googlechartid_chart_1111. Accessed 31 Jan 2022
 68. Commission E (2018) Renewable Energy – Recast to 2030 (RED II). https://joint-research-centre.ec.europa.eu/welcome-jec-website/reference-regulatory-framework/renewable-energy-recast-2030-red-ii_en. Accessed 24 Mar 2022
 69. De Jong S, Antonissen K, Hoefnagels R, Lonza L, Wang M, Faaij A, Junginger M (2017) Life-cycle analysis of greenhouse gas emissions from renewable jet fuel production. *Biotechnol Biofuels* 10:64. <https://doi.org/10.1186/s13068-017-0739-7>
 70. Phillips R, Dunnill Charles W (2016) Zero gap alkaline electrolysis cell design for renewable energy storage as hydrogen gas. *RSC Adv* 6:100643–100651. <https://doi.org/10.1039/c6ra22242k>
 71. European Commission (2022) Hydrogen: commission supports industry commitment to boost by tenfold electrolyser manufacturing capacities in the EU https://ec.europa.eu/commission/press-corner/detail/en/ip_22_2829. Accessed 8 Dec 2022

Publisher's note Springer Nature remains neutral with regard to jurisdictional claims in published maps and institutional affiliations.